Temperature Excursions in Catalytic Monoliths

L. LOUIS HEGEDUS

General Motors Research Laboratories
Warren, Michigan 48090

The application of monolithic catalysts to automotive emission control has frequently been complicated by unexplained thermal degradation phenomena. This paper reports experimental and theoretical studies aimed at the understanding of how heat is generated and distributed in catalytic monoliths during an exothermal, mass transfer limited reaction.

Theoretical considerations indicate that under certain operating conditions the steady state solid catalyst temperature can exceed the adiabatic reaction temperature. It is also shown that the catalyst overtemperature is influenced by the nature of the reactive species and by the geometry of the catalyst. These predictions have been verified by experiments in a novel tubular reactor.

SCOPE

Monolithic (that is, one-piece) catalyst supports were first proposed for automobile catalytic applications by Johnson et al. (1961). Since their inception they have been considered to be promising for catalytic applications where high volumetric flow rates are coupled with the requirement of low pressure drops. The one-piece construction offers attrition-free operation in a vibrating and pulsating atmosphere and also offers a great deal of design flexibility due to the variety of geometric configurations which can be conceived (for example, Hegedus, 1973). However, monolithic catalysts in oxidative automotive converters have been frequently plagued by thermal excursions which can deteriorate or even melt these catalysts (for example, Morgan et al., 1973). The aim of this paper is to investigate the generation and distribution of heat in catalytic monoliths during a steady state exothermic chemical reaction. The hope is that an understanding of the reasons behind the overtemperature phenomena will allow us to design monoliths which are less prone to thermal degradation.

In the subsequent parts, a mass transfer limited steady state mathematical model is presented. Emphasis is given to first-order effects and thus to relative simplicity. The implications of the mathematical analysis are experimentally investigated using reactors which were designed to allow the simultaneous mapping of gas and solid temperatures along the reactor axis. In particular, propylene, carbon monoxide, and hydrogen, which represent the major combustible species in automobile exhaust, were oxidized in experimental monoliths with square and equilateral triangular channel geometries.

CONCLUSIONS AND SIGNIFICANCE

Semiquantitative calculations and laboratory experiments indicate that the magnitude of the solid overtemperature is influenced by the nature of the oxidizable species and by the channel geometry of the monolithic catalysts.

For propylene, the solid temperature stays below the adiabatic reaction temperature along the entire length of the catalyst, gradually increasing from its initial value at the reactor entrance toward the adiabatic reaction temperature. For carbon monoxide, the solid temperature stays nearly constant along the length of the monolith and it has the value of the adiabatic reaction temperature. The most interesting case is the oxidation of hydrogen. As predicted by the theory, the experiments showed solid temperatures which exceeded the adiabatic reaction temperature. The solid temperature is highest near the reactor entrance, and it gradually decreases to the adiabatic reaction temperature along the reactor's length.

The shape of the monolith channels also influences the solid overtemperature. For example, triangular monolith channels were found to result in somewhat lower solid overtemperatures than square channels under comparable conditions.

These observations have direct implications for the operation of automotive converters where the exhaust gas composition changes with the operating mode of the engine. Thus, overload (high H_2 and CO, low hydrocarbon concentrations) will result in solid temperatures which exceed adiabatic and ignition failure (low H_2 and CO, but high hydrocarbon concentrations) will result in solid temperatures which do not exceed the adiabatic reaction temperature.

SIMPLEST HETEROGENEOUS MODEL*

Let us first consider a classical model which assumes plug flow in the gas phase, complete external mass transfer limitations (that is, the concentration of the reactant at the surface of the monolith is essentially zero) and zero axial heat conductivity both in the solid and in the gas phase. For species $i = 1 \ldots n$, the conservation of energy and mass can be expressed by

$$\frac{d\Theta_g}{d\xi} - \alpha(\Theta_s - \Theta_g) = 0 \qquad (1)$$

$$(\Theta_s - \Theta_g) - \sum_{i=1}^{n} \beta_i \Psi_i = 0 \qquad (2)$$

* A more detailed version of this section has been deposited as a supplement as Document No. 02641 with the National Auxiliary Publications Service (NAPS), c/o Microfiche Publications, 440 Park Ave. S., New York, N. Y. 10017 and may be obtained for $1.50 for microfiche or $5.00 for photocopies.

$$\frac{d\Psi_i}{d\xi} + \gamma_i \Psi_i = 0, \quad i = 1 \ldots n \tag{3}$$

$$\Theta_g(0) = 1 \tag{4}$$

$$\Psi_i(0) = 1, \quad i = 1 \ldots n, \quad \text{where} \tag{5}$$

$$\Theta_g = \frac{T_g}{T_0} \tag{6}$$

$$\Theta_s = \frac{T_s}{T_0} \tag{7}$$

$$\Psi_i = \frac{c_i}{c_{0,i}}, \quad i = 1 \ldots n \tag{8}$$

$$\xi = \frac{x}{L} \tag{9}$$

$$\alpha = \frac{s_g \bar{h} L}{v \rho C_p} \tag{10}$$

$$\beta_i = \frac{\bar{k}_i c_{0,i}(-\Delta H_i)}{\bar{h} T_0} \tag{11}$$

$$\gamma_i = \frac{s_g \bar{k}_i L}{v}, \quad i = 1 \ldots n \tag{12}$$

Equations (1) to (5) can be easily solved and the results are

$$\Psi_i = \exp\{-\gamma_i \xi\}, \quad i = 1 \ldots n \tag{13}$$

$$\Theta_g = 1 + \alpha \sum_{i=1}^{n} \frac{\beta_i}{\gamma_i} (1 - \exp\{-\gamma_i \xi\}) \tag{14}$$

$$\Theta_s = \Theta_g + \sum_{i=1}^{n} \beta_i \exp\{-\gamma_i \xi\} \tag{15}$$

The adiabatic reaction temperature at complete conversion is expressed by

$$\Theta_{ad} = 1 + \alpha \sum_{i=1}^{n} \frac{\beta_i}{\gamma_i} \tag{16}$$

It refers to the dimensionless temperature of the exhaust from an infinitely long, adiabatic reactor.

Let us now analyze the solutions (13) to (15). First, the dimensionless gas temperature is expected to stay below the adiabatic reaction temperature in all cases [Equations (14) and (16)]. The solid temperature can be expressed from (14) to (16) as

$$\Theta_s = \Theta_{ad} + \sum_{i=1}^{n} \beta_i \left(1 - \frac{\alpha}{\gamma_i}\right) \exp\{-\gamma_i \xi\} \tag{17}$$

Inspection of this expression reveals that the nature of the solid temperature distribution with respect to the gas temperature distribution and the adiabatic reaction temperature is determined by the ratio α/γ_i.

Depending on whether $\alpha > \gamma_i$ or $\alpha < \gamma_i$, the solid temperature can be smaller or larger than the adiabatic reaction temperature.

The difference between the solid and gas temperatures is largest near the reactor entrance:

$$\Theta_s(0) = 1 + \sum_{i=1}^{n} \beta_i \tag{18}$$

Thus, the magnitude of β_i is characteristic of the largest solid temperature above the input gas temperature and the magnitude of α/γ_i determines the relative position of Θ_s with respect to the adiabatic reaction temperature:

$$\frac{\Theta_s(0)}{\Theta_{ad}} = \frac{1 + \sum_{i=1}^{n} \beta_i}{1 + \alpha \sum_{i=1}^{n} \frac{\beta_i}{\gamma_i}} \tag{19}$$

Let us now inspect α/γ_i and β_i and determine the parameters that influence their magnitudes.

Heat and mass transfer coefficients are conveniently expressed from

$$Nu = \frac{2R\bar{h}}{k_{T,g}} \quad \text{(Nusselt number)} \tag{20}$$

$$Sh_i = \frac{2R\bar{k}_i}{D_i} \quad \text{(Sherwood number)} \tag{21}$$

In the case of completely external mass transfer limited reactions in catalytic monoliths, the mass transfer problem can be approximated by taking a constant (that is, zero) surface composition, which corresponds to a heat transfer problem with constant surface temperature. Thus, the mass transfer coefficients can be calculated from the appropriate heat transfer analogy using the T type boundary condition (Rolke et al., 1972).

The proper boundary condition for the simultaneous heat transfer problem is probably much different. One can specify either the wall temperature distribution or the wall heat flux distribution. The physical properties of monoliths used in subsequent experiments suggest that the steady state heat transfer problem might be better approximated by assuming that the thermal conductivity of the wall is zero in the axial direction (heat conducted in the wall in the axial direction is negligible compared with the heat convected by the gas stream) and infinite in the direction perpendicular to the flow (uniform radial solid temperature profile). This corresponds to the $H1$ boundary condition. [In transient heat transfer experiments (Heck et al., 1974), an intermediate situation might prevail].

Solutions for the Nusselt numbers at these boundary conditions in straight channels of various cross sections have been published (Shah and London, 1971) and allow us to approximate the heat and mass transfer coefficients in the monoliths.

For fully developed laminar flows,

$$Nu = Nu_{\infty,H1} \tag{22}$$

$$Sh_i = Nu_{\infty,T} \tag{23}$$

with

$$Sc_i = \frac{\mu}{\rho D_i} \quad \text{(Schmidt number)} \tag{24}$$

and

$$Pr = \frac{C_P \mu}{k_{T,g}} \quad \text{(Prandtl number)}, \tag{25}$$

$$\frac{\alpha}{\gamma_i} = \left(\frac{k_{T,g}}{D_i \rho C_P}\right)\left(\frac{Nu_{\infty,H1}}{Nu_{\infty,T}}\right) = \left(\frac{Sc_i}{Pr}\right)\left(\frac{Nu_{\infty,H1}}{Nu_{\infty,T}}\right) = Le_i\left(\frac{Nu_{\infty,H1}}{Nu_{\infty,T}}\right) \tag{26}$$

$$\beta_i = \left(\frac{D_i}{k_{T,g} \rho C_P}\right)\left(\frac{c_{0,i}(-\Delta H_i)}{T_0}\right)\left(\frac{Nu_{\infty,T}}{Nu_{\infty,H1}}\right) \tag{27}$$

Thus, the maximum difference between solid and gas

temperature and the relative position of the solid temperature with respect to the adiabatic reaction temperature are influenced both by the nature of the oxidizable species i and by the geometry of the catalyst. In particular, β_i will be larger for a species having a higher diffusivity, or a higher heat of combustion, or a higher inlet concentration. The ratio α/γ_i influences the solid temperature distribution in an interesting way. Qualitatively different situations might arise under various conditions which are characteristic to the operation of automotive converters. For hydrocarbons such as propylene, it is estimated that $\alpha > \gamma_i$, which means that the solid temperature will always stay below the adiabatic reaction temperature. For hydrogen, in turn, it is expected that $\alpha < \gamma_i$, that is, the solid temperature will exceed the adiabatic reaction temperature and this will happen near the reactor entrance. Calculations for CO indicate that α/γ_i will be somewhat below unity but very close to it so that the solid temperature should stay very close to the adiabatic reaction temperature along the entire length of the reactor.

The effects of monolith geometry on solid overtemperatures are reflected by the trends in the ratio $Nu_{z,H1}/Nu_{z,T}$. The higher this ratio, the lower β_i and higher α/γ_i is expected to be, that is, the less solid overtemperature should occur. The trend of the $Nu_{z,H1}/Nu_{z,T}$ ratios follows an opposite trend to that of the $Nu_{z,T}$ values which in turn reflect the conversion efficiency for the various monolith geometries.

EXPERIMENTAL REACTORS

The theoretical possibility that the solid temperature can exceed the adiabatic reaction temperature in steady state catalytic gas-solid systems has been pointed out by several authors (for example, Satterfield et al., 1954; Carberry and Kulkarni, 1973; Heck, 1974). Axial solid temperature profiles in tubular reactors with catalytic walls were actually measured by Satterfield et al. (1954). For the particular reactive system they chose, the solid temperature remained below adiabatic. The high thermal conductivity of the metal catalyst tube had a significant effect on the shape of the axial solid temperature distribution. In addition, the solid temperature measurements were discontinuous (localized) and no gas temperature profiles were obtained.

In this paper tubular ceramic catalytic reactors will be described which allow the simultaneous and continuous mapping of gas and solid catalyst temperatures along the reactor axis while a mass transfer limited catalytic reaction is occurring on the walls.

Figure 1 shows the construction of monolithic reactors which were used in the experiments. Extruded cordierite $[(MgO)_2\ (Al_2O_3)_2\ (SiO_2)_5]$ monoliths with two different channel cross-sectional geometries were sculptured so that

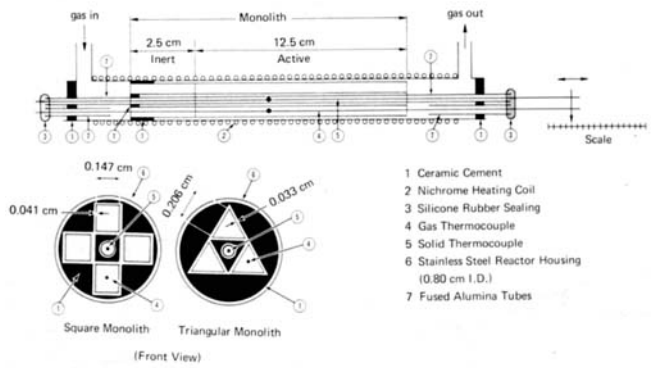

Fig. 1. Schematic representation of the monolithic reactors (dimensions not in proportion). Note the sliding thermocouples for solid and gas temperature measurements.

several channels symmetrically surround a central channel. A thin fused alumina tube fills the central channel (sealed to it by ceramic cement). The ends of this tube protrude from the gas flow. A 0.013-cm diameter iron-constantan thermocouple is fed through the alumina tube such that the welding point is in the middle of the wire. This thermocouple is situated in a stagnant gas field and at steady state it will assume the temperature of the surrounding solid. The ends of the fused alumina tubes are sealed with a self-hardening silicone rubber seal which effectively holds the thermocouple wire in place and allows it to be moved back and forth along the reactor axis without gas leakage from the reactor.

The reaction occurs in the channels which surround the central channel. The monolith walls are coated by about 10 wt % gamma alumina which in turn is impregnated with a $H_2(PtCl_6)$ solution to yield a final Pt content of about 1.5% of the alumina. Electron microprobe scans were used to check the uniformity of the Pt distribution along the channel axis.

In order to reduce the effects of developing flows on the heat and mass transfer coefficients, a 2.5-cm long section of the monolith was left unimpregnated. This was achieved by cementing a 2.5-cm long unimpregnated monolith section to the front of the impregnated monolith.

The gas temperature in the reactive monolith channels is measured by a sliding thermocouple which is similar in construction to the solid thermocouple. A 0.013-cm diameter iron-constantan thermocouple is fed through one of the reactive channels. The ends of this thermocouple are fed through fused alumina tubes at the ends of the reactor. This thermocouple also passes through a silicone rubber seal at both ends. At high temperatures, the gas temperature readings might be influenced somewhat by radiation from the surrounding monolith walls.

The monolith is inserted into a 0.80-cm inner diameter stainless steel tube. At the inlet end, the monolith is cemented to the tube by ceramic cement. The other end stays free so that the steel tube and the monolith can expand independently at high temperatures (the steel tube has a much higher thermal expansion coefficient than cordierite).

The reactor is heated by a nichrome wire coil winding. The wire is insulated by a heat resistant woven glass tube insulator. To reduce heat loss from the monolith, the temperature of the stainless steel reactor housing is kept at the adiabatic reaction temperature of the particular experiment and the reactor was heavily insulated from the ambient.

The position of the welding points of the sliding thermocouples is monitored with respect to a millimeter scale during the experiments.

The reactor is supplemented by nondispersive infrared CO and CO_2 analyzers, a polarographic O_2 analyzer, a flame ionization hydrocarbon analyzer, and a thermal conductivity hydrogen analyzer.

The feed gas contained about 6 mole % O_2 and various amounts of H_2, CO, or propylene so that the adiabatic temperature rise was easily measurable but not excessive. The balance of gas was provided by N_2 as diluent. The flows of the individual gases were metered by precision rotameters, while the total gas flow rate was monitored by a thermistor gas flow meter.

Pressures at various points of the system were measured by a precision Bourdon gauge.

The reaction mixture was preheated by passing it through a silicon carbide-filled preheater oven. Since a certain degree of conversion of the oxidizable species always occurred in the preheater, the feed gas was sam-

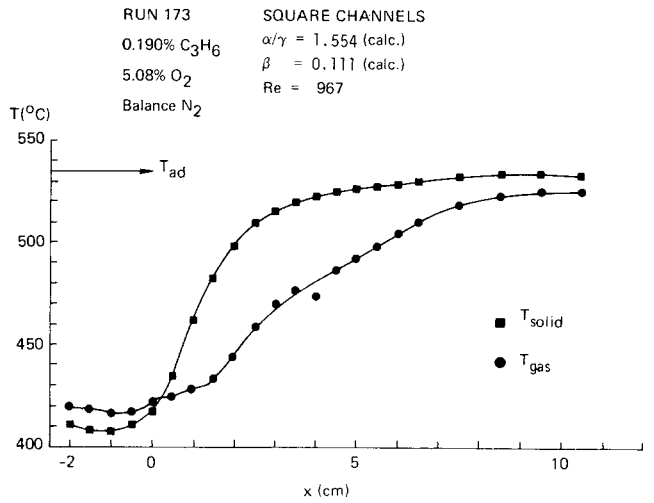

Fig. 2. Oxidation of propylene in a monolith with square channels.

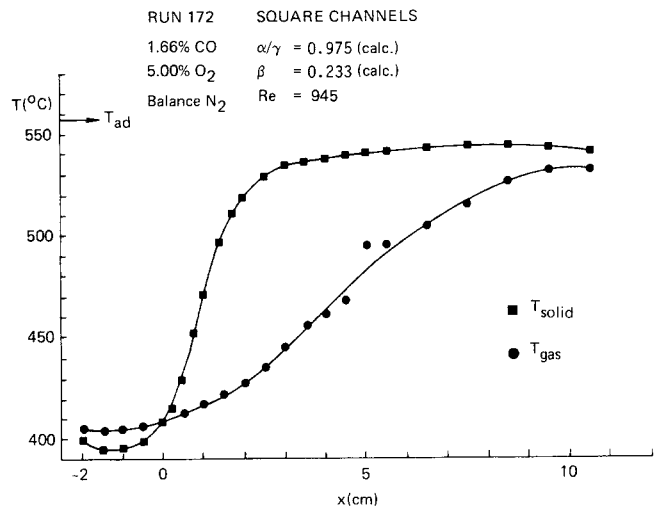

Fig. 3. Oxidation of carbon monoxide in a monolith with square channels.

pled at the monolith reactor entrance. This allowed the measurement of concentrations actually entering the reactor.

RESULTS AND DISCUSSION

Hydrogen, carbon monoxide, and propylene were oxidized in the reactors described in the previous chapter. The flow rate and temperature were varied until complete mass transfer control for the particular reaction was attained. Typically, a measured conversion which was independent of the reaction temperature served as an indication of mass transfer control.

Let us first discuss the effects of the reactive species on the solid and gas temperature distribution. Figure 2 shows temperature profiles for the oxidation of propylene in a square channeled monolith (Figure 1). The calculated value of α/γ_i for this experiment is well above unity. Accordingly, we expect the gas and solid temperatures to stay below adiabatic along the reactor's length. As Figure 2 shows, this is indeed the case.

Figure 3 is the result of a CO oxidation experiment, also under mass transfer controlled conditions. α/γ_i is very close to unity but somewhat below it. Consequently, the solid temperatures will stay near the adiabatic reaction temperature, as the experiments verified. The solid temperature rises more rapidly than in Figure 2 and stays closer to the adiabatic reaction temperature along the monolith's length.

The most interesting data are shown in Figure 4 which displays the results of hydrogen oxidation experiments in square channeled monoliths. For this experiment, it is calculated that $\alpha/\gamma_i < 1$ which dictates that the solid temperature should exceed the adiabatic reaction temperature and approach it from above as we progress along the monolith's axis. This indeed occurred during the experiment. The initial rise near the entrance is due to the finite heat conductivity of the cordierite from the reactive section of the monolith to the attached inert inlet section.

Figure 5 shows the combined effects of CO and H_2 on the temperature profiles. The net result is a slightly higher than adiabatic solid temperature in the monolith. Again, the solid temperature near $x = 0$ is reduced due to the finite conductivity of the cordierite. To investigate this effect, H_2 oxidation experiments were conducted in a monolith which did not have an inert inlet section. No maximum was observed in those experiments. Instead, the solid temperature monotonically decreased from its high-

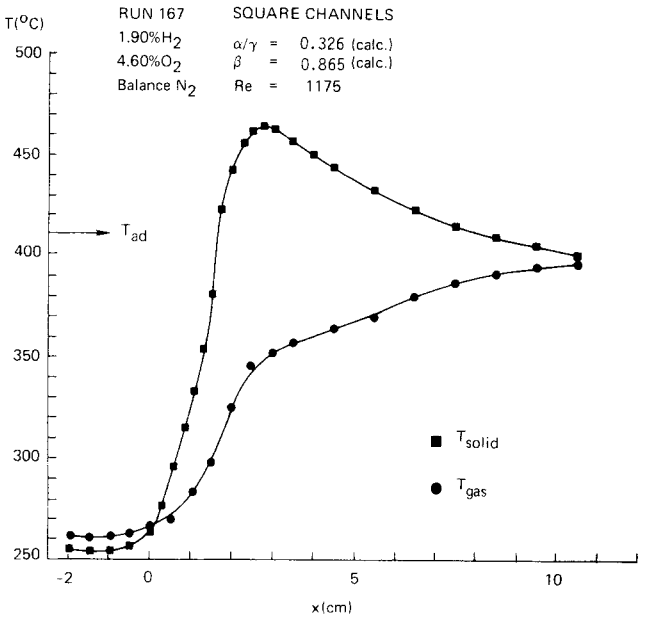

Fig. 4. Oxidation of hydrogen in a monolith with square channels.

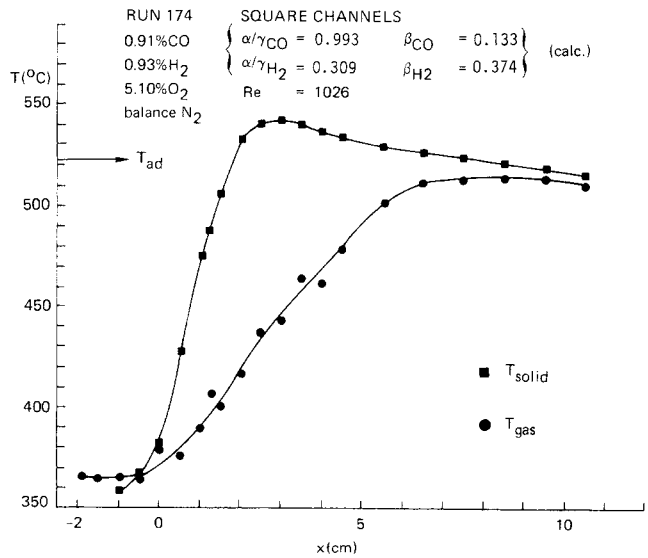

Fig. 5. Oxidation of a mixture of hydrogen and carbon monoxide in a monolith with square channels.

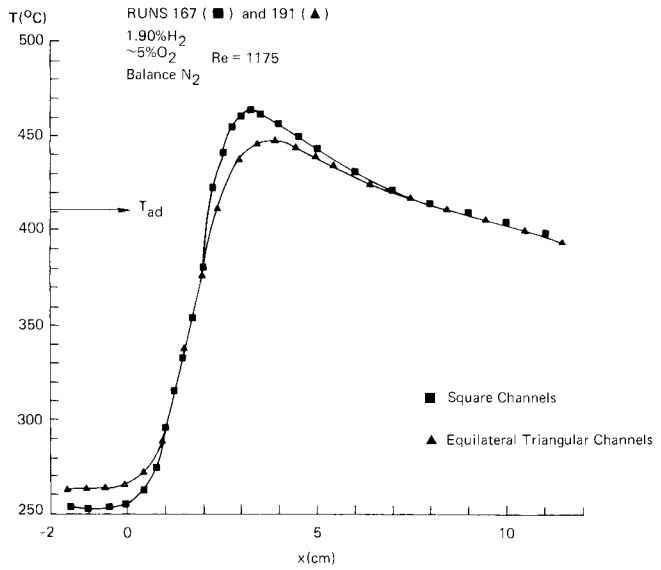

Fig. 6. Comparison of the solid temperatures during the oxidation of hydrogen in monoliths with square and equilateral triangular channels at equal Reynolds numbers.

est value at $x = 0$, approaching the adiabatic reaction temperature from above as our simple model predicted.

In addition to the square monolith channels, monoliths with other geometries were also used for the oxidation of hydrogen, carbon monoxide, and propylene. The effects of the oxidizable species on the qualitative nature of the temperature distributions in these additional geometries were similar to the effects described above for the square channeled monolith.

Previous theoretical considerations in this paper indicated that the magnitude of the solid overtemperature is determined by β_i [Equation (17)] and that β_i depends on the nature of the oxidizable species and on the monolith geometry [Equation (27)]. For the same species and equivalent reaction conditions, overtemperature should be increasingly severe as $Nu_{x,H1}/Nu_{x,T}$ decreases with changing geometry. Our purpose is now to check experimentally whether this qualitative trend is correct.

Two channel geometries will be considered here: square and equilateral triangle. The comparison of the overtemperature behavior of monoliths with these channel geometries is of interest in automotive exhaust control practices.

The monoliths were compared at equal Reynolds numbers. Both had a 2.5-cm inert inlet section to eliminate developing flow effects. The concentrations of the oxidizable species and the input gas temperature were the same in both experiments.

Figure 6 shows the comparison of the two monoliths for the oxidation of hydrogen. As our semiquantitative calculations predict, overtemperature is somewhat less severe in the monolith with triangular channels.

ACKNOWLEDGMENT

The author acknowledges the technical help of J. Melbardis who built the reaction apparatus and conducted the experiments.

NOTATION

c_i = concentration of species i, mole/cm^3
$c_{0,i}$ = concentration of species i at the reactor entrance, mole/cm^3
C_P = heat capacity of the reaction mixture, cal/g/°C
D_i = diffusivity of species i, cm^2/s
$\bar{h}$ = heat transfer coefficient, cal/cm^2/s/°C
ΔH_i = heat of combustion of species i, cal/mole
$\bar{k}_i$ = mass transfer coefficient of species i, cm/s
$k_{T,g}$ = thermal conductivity of the reaction mixture, cal/cm/s/°C
L = length of the monolith, cm
Le_i = Lewis number, see text
Nu = Nusselt number, see text
$Nu_{x,H1}$ = fully developed Nusselt number with $H1$ boundary conditions, see text
$Nu_{x,T}$ = fully developed Nusselt number with T boundary conditions, see text
Pr = Prandtl number, see text
R = hydraulic radius (twice the geometric cross section area, divided by the wetted perimeter), cm
s_g = surface to volume ratio (geometric surface divided by the void volume), (cm^2/cm^3) $= 2/R$
Sc_i = Schmidt number of species i, see text
Sh_i = Sherwood number of species i, see text
T_{ad} = adiabatic reaction temperature, °K
T_g = gas temperature, °K
T_s = solid temperature, °K
T_0 = gas temperature at reactor entrance, °K
v = interstitial gas velocity, cm/s
x = monolith length coordinate, cm

Greek Letters

α = dimensionless constant, see text
β_i, γ_i = dimensionless constants, see text
Θ_{ad} = dimensionless adiabatic reaction temperature
Θ_g = dimensionless gas temperature
Θ_s = dimensionless solid temperature
μ = viscosity of the reaction mixture, g/cm/s
ξ = dimensionless monolith length coordinate
ρ = density of the reaction mixture, g/cm^3
Ψ_i = dimensionless concentration of species i

LITERATURE CITED

Carberry, J. J., and A. A. Kulkarni, "The Non-isothermal Effectiveness Factor for Monolith Supported Catalysts," *J. Catalysis*, **31**, 41 (1973).

Heck, R. H., "Heat Transfer and Reaction Modeling in Monolithic Catalysts," Ph.D. dissertation, Univ. Delaware, Newark (1974).

Heck, R. H., J. Wei, and J. R. Katzer, "The Transient Response of a Monolithic Catalyst Support," *Adv. Chem. Ser.*, **133**, 34 (1974).

Hegedus, L. L., "Effects of Channel Geometry on the Performance of Catalytic Monoliths," Preprints of the Petroleum Div., Am. Chem. Soc., **18**, 487 (1973).

Johnson, L. I., W. C. Johnson, and D. L. O'Brien, "The Use of Structural Ceramics in Automobile Exhaust Converters," *Chem. Eng. Progr. Symp. Ser.*, **35**, 55 (1961).

Morgan, C. R., D. W. Carlson, and S. E. Voltz, "Thermal Response and Emission Breakthrough of Platinum Monolithic Catalytic Converters," paper presented at meeting Soc. Automotive Engrs., Detroit (1973).

Rolke, R. W., R. D. Hawthorne, C. R. Garbett, E. R. Slater, T. T. Phillips, and G. D. Towell, "Afterburner Systems Study," EPA-R2-72-062, Environmental Protection Agency, (1972).

Satterfield, C. N., H. Resnick, and R. L. Wentworth, "Simultaneous Heat and Mass Transfer in a Diffusion-Controlled Chemical Reaction," *Chem. Eng. Progr.* **50**, 460 (1954).

Shah, R. K., and A. L. London, "Laminar Flow for Forced Convection Heat Transfer and Flow Friction in Straight and Curved Ducts—A Summary of Analytical Solutions," Techn. Report No. 75, Stanford Univ., (1971).

Manuscript received January 16, 1975; revision received March 17 and accepted March 27, 1975.